The Generation of Antimicrobial Peptide Activity: A Trade-off between Charge and Aggregation?**

Marc Torrent, Javier Valle, M. Victòria Nogués, Ester Boix, and David Andreu

Antimicrobial peptides (AMPs) are innate immune system effectors with a vital role in the prevention of infection. Despite being actively researched in recent years for their potential therapeutic application against infectious diseases,[1] the molecular mechanisms by which AMPs exert their activity are not fully understood, although they clearly involve membrane binding and destabilization as a common essential step.[2] It is also well known that amphipathic structures, such as those of the typical AMPs magainin and cecropin, are favored for membrane binding and pore formation.[3]

Interestingly, AMPs such as bacteriocins[4] and temporins,[5] or proteins like lysozyme,[6] lactoferrin,[7] and eosinophil cationic protein,[8] have recently been described to form amyloid-like structures. In addition, many amyloid proteins share with AMPs membrane-perturbing abilities such as binding to negatively charged membranes[9] or preference for liquid disordered domains.[10] For instance, amyloid-forming proteins, such as prion protein and amyloid-β protein, can destabilize phospholipid bilayers[11] and have even been described to possess some antimicrobial activity.[12] It has indeed been suggested that dementia and amyloid deposits that induce brain-barrier permeabilization and atrophy might result from lipopolysaccharide or other debris left over from previous bacterial infection.[13] All this evidence could be used to hypothesize that amyloid propensity and antimicrobial activity are related in the sense that aggregation-prone regions may have served as templates from which AMPs were evolutionarily derived.

To identify structural features common to both amyloid and antimicrobial regions, we analyzed the amino acid frequency in amyloid-prone regions[14] and AMPs. Our inspection revealed that, for 80% of amino acid residues, there is a coincident tendency to be present in (or absent from) both antimicrobial and amyloid-like regions (Figure 1a). The good correlation between both tendencies suggests that they may be somehow related. Even more, the residue-intrinsic propensities for both properties, that is, the probability for an individual residue to be located in either aggregation-prone[15] or antimicrobial domains,[16] are also well correlated (Figure 1b). The main exceptions to this concurrent behavior were positively charged residues, favored in antimicrobial but detrimental in aggregation-prone regions.
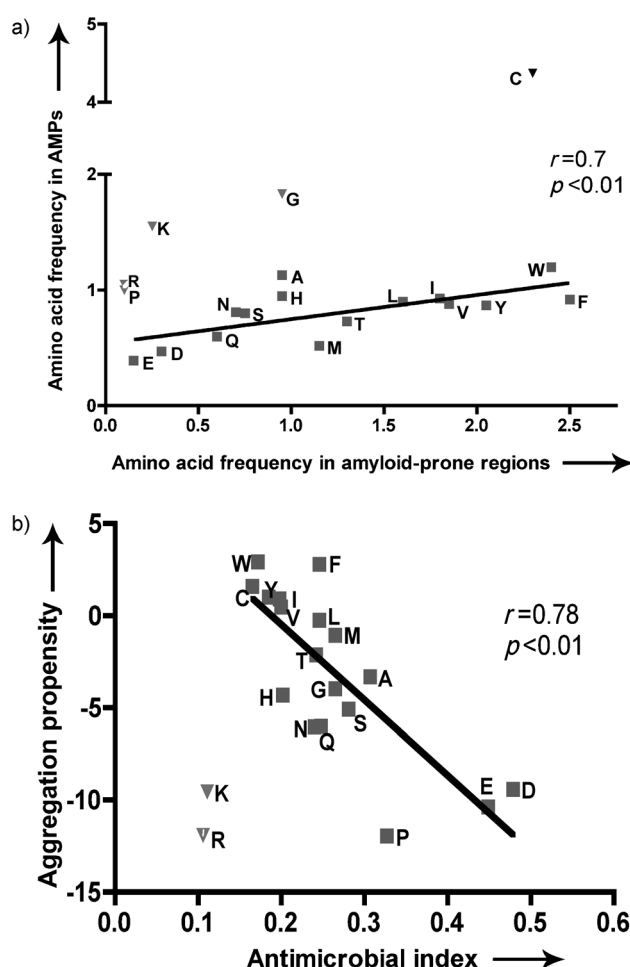

Figure 1. Aggregation and antimicrobial relationships. a) Frequency and b) aggregation versus antimicrobial propensity are plotted for amino acid residues in amyloid-prone regions and AMPs. Well-correlated and outlying residues are shown as squares and inverted triangles, respectively. Amino acid frequencies in amyloid-prone regions were obtained from Ref. [14], and in AMPs as detailed in the Supporting Information. Aggregation propensity values are from Ref. [15] and antimicrobial index from Ref. [16]. *p* values are in all cases < 0.01.

[*] Dr. M. Torrent, J. Valle, Prof. D. Andreu
Department of Experimental and Health Sciences
Universitat Pompeu Fabra
Dr. Aiguader 88, 08003 Barcelona (Spain)
E-mail: david.andreu@upf.edu
Prof. M. V. Nogués, Dr. E. Boix
Department of Biochemistry and Molecular Biology
Universitat Autònoma de Barcelona, Biosciences Faculty
Building C, 08193 Barcelona (Spain)

The outlier behavior of Pro, Gly, and Cys in Figure 1 a can arise from the number of annotated AMPs rich in these three amino acids. From these results it is appealing to hypothesize that insertion of cationic residues at privileged points in amyloid-prone sequences could not only disrupt the amyloid-forming tendency of those regions but also, in favorable (membrane-like) environments, promote amphipathic structuring and AMP behavior.

From an evolutionary perspective, inspection of AMP sequence properties from bacteria to humans reveals several interesting conclusions (Figure 2). 1) Whereas mean positive charge increases from bacteria ($+2, +3$) to humans ($+6, +7$), aggregation displays the opposite trend, with human AMPs showing the minimal propensity. 2) Despite the mean rise in charge from bacterial to mammalian AMP sequences, Lys remains the dominant cationic residue in all AMP groups until late stages (bacteria to fish). Henceforth, Arg becomes more favorable and the highest Arg:Lys ratios are reached (from birds to mammals). These patterns observed for AMPs are not paralleled by non-AMPs (Supporting Information, Figure S1), for which aggregation and charge remain roughly constant through evolution, with the exception of fish, and where R:K ratios are similar for bacteria, plant, and avian groups.

These evolutionary data are congruent with our above hypothesis for amyloid-to-antimicrobial transition. A similar scenario has been invoked for new antimicrobial strategies emerging upon phagocyte appearance[18] (Figure 1 c), based on pathogen internalization in vesicles containing cytotoxic AMPs. The much later emergence of adaptive, increasingly complex immune systems would seem to coincide with structural modifications such as the α-γ-β motif[18] in γ-core-containing peptides. A diversification of targets and functions (e.g., intracellular targeting[19]) of most AMPs could also con-

tribute to the overrepresentation of Arg residues.[20] These considerations can be regarded as supporting the hypothesis (Figure 2 a) that cationization at appropriate points may provide a mechanism whereby aggregation-prone sequences can be turned into AMPs.

To validate this point, 14 proteins described to form amyloid aggregates were selected and analyzed by four
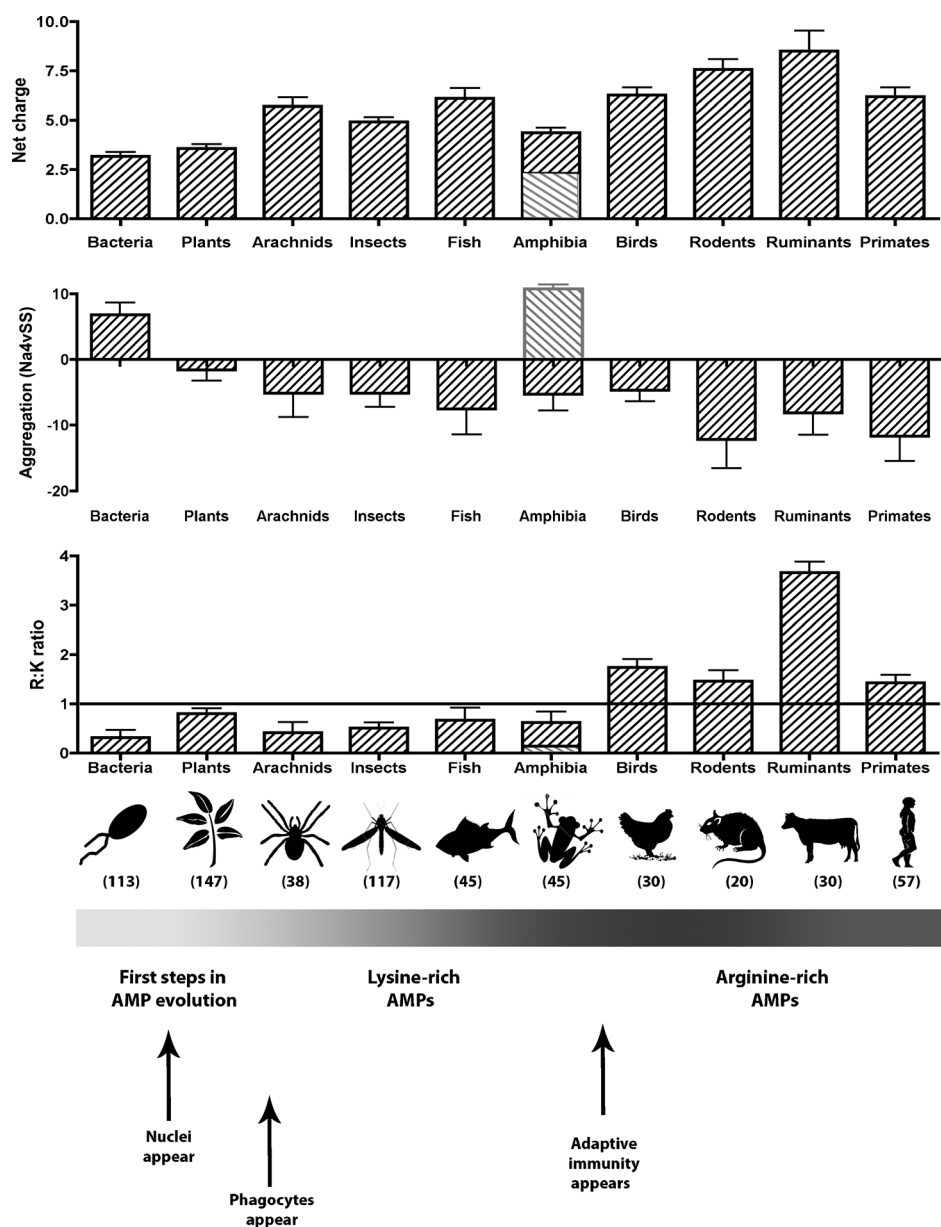

Figure 2. An AMP evolutionary scenario. AMPs from all groups of organisms follow opposite trends with regard to net charge (top) and aggregation propensity (middle); $p < 0.001$. Normalized a4v sequence sum (Na4vSS) values represent the average aggregation propensity over the entire sequence divided by the number of residues and multiplied by 100.[17] Amphibian AMPs follow the trend only if internal (that is, not skin-secreted) peptides are considered. If all amphibian AMPs (lighter shaded bars) are considered, the trend found for all other groups of organisms is not kept, perhaps reflecting a specialized role of AMPs in amphibian skin, where aggregation/concentration effects are less harmful than on other AMP-producing organs. Cationic character (bottom) is predominantly due to Lys residues in the first six AMP groups (white-to-dark gray bars) whereas in the rest (birds to primates, dark-to-lighter gray bars) Arg predominates as cationic residue, which coincides with the emergence of adaptive immune responses. The results were found statistically significant under the Fisher test.

aggregation-predicting algorithms (Supporting Information, Table S1). This analysis allowed selection of 24 15-residue peptides with optimized coverage of predicted amyloid-forming regions (Supporting Information, Figure S2) that were used as templates for amyloid-derived AMP (ADAMP) generation.

As a criterion for cationization, the fact that certain residues are preferentially incorporated at given positions rather than randomly along a peptide sequence was taken into account. For Lys in particular, and using a 15-residue frame, positions 7, 12, and 15 are described as the most favored in imparting amphipathic properties to the peptide[21] (Support-

ing Information, Figure S3). On this basis, the 24 amyloid-prone 15-mers were converted into ADAMPs by Lys cationization at privileged positions 7, 12, and 15 (Table 1 and Supporting Information, Table S2).

Next, sequences resulting from this cationization process were screened for antimicrobial activity using a support vector machine algorithm[22] (Supporting Information, Table S2), which showed that about 75% of (originally amyloid-prone) cationized regions could be predicted as putative ADAMPs. In contrast, neither the amyloid parental sequences (Supporting Information, Table S2) nor 24 random (RP), nor 22 non-amyloid (NAP) sequences were predicted as antimicrobial when submitted to cationization (Supporting Information, Tables S3 and S4).

For experimental validation of the hypothesis, the 24 ADAMPs were synthesized and tested for antimicrobial activity (Table 1) and secondary structure (Figure 3b). A broad majority of ADAMPs (75%, assuming a fairly strict threshold of 10 µM, Table 1) displayed relevant activity on both Gram-negative (*Escherichia coli*) and Gram-positive (*Micrococcus luteus*) bacteria, in good agreement with the computational prediction. Also screened for antimicrobial activity was a panel of 14 control peptides containing both RP and NAP sequences, as well as their cationized versions (CRP and CNAP, respectively). Setting 10 µM as a threshold of

Table 1: Antimicrobial activity[a] of ADAMPs[b] and control peptides.[c]

Peptide	Sequence	MIC$_{50}$ (*E. coli*)[d]	MIC$_{50}$ (*M. luteus*)[d]
ADAMP1	SNNFGAKLSSTKVGK	6.3	5.3
ADAMP2	SNKGAIKGLMVKGVK	0.6	0.9
ADAMP3	VTNVGGKVVTGKTAK	4.3	4.9
ADAMP4	GAAAAGKVVGGKGGK	2.7	3.3
ADAMP5	ALLSPYKYSTTKVVK	1.3	0.4
ADAMP6	GKSNFLKSYVSKHPK	0.2	0.6
ADAMP7	SQSSVDKLNWYKQRK	0.7	1.6
ADAMP8	GKAPKLKIFDTKNLK	0.4	0.6
ADAMP9	RSGTDFKLTISKLQK	0.7	0.8
ADAMP10	PDDFATKYSQQKYTK	7.3	2.2
ADAMP11	SNGPVKKWGSIKGLK	0.7	2.3
ADAMP12	DVSIEDKVISLKGDK	>100	>100
ADAMP13	HSIIGRKLVVHKKAK	0.1	0.3
ADAMP14	KHGATVKTALGKILK	0.3	0.4
ADAMP15	VKYLEFKSESIKQVK	16.3	14.4
ADAMP16	DMQSLFKQYFQKMTK	1.6	2.5
ADAMP17	AGTSLVKFFSSKMNK	1.8	2.0
ADAMP18	LPGSSKKFSVYKDQK	15.8	19.2
ADAMP19	TSLGGWKLIQQKMDK	77.1	>100
ADAMP20	GNDYLHKLTQRKSVK	2.4	4.3
ADAMP21	EIENGVKWVSFKGAK	34.5	20.1
ADAMP22	YTGIFTKQVLSKLKK	0.3	0.9
ADAMP23	GSHLVEKLYLVKERK	5.6	5.1
ADAMP24	GISLANKMSLAKWEK	50.4	56.7
RP1	DEKIYLIKVADVDQR	>100	>100
RP2	LMEIHHRASQDTPKE	>100	>100
RP3	WYADHSDQYQLLDTP	>100	>100
RP5	DLVELAMLEADRMSR	>100	>100
RP11	QDNYWVTQGLNILSG	>100	>100
CRP1	DEKIYLKKVADKDQK	>100	>100
CRP2	LMEIHHKASQDKPKK	>100	>100
CRP3	WYADHSKQYQLKDTK	>100	>100
CRP5	DLVELAKLEADKMSK	>100	>100
CRP11	QDNYWVKQGLNKLSK	100	25
NAP1	TPIESHQVEKRKSNT	>100	>100
NAP2	MHMNVQNGKWDSDPS	>100	>100
CNAP1	TPIESHKVEKRKSNK	100	100
CNAP2	MHMNVQKGKWDKDPK	>100	>100

[a] Antimicrobial activity is expressed as the minimum inhibitory concentration at 50% (MIC$_{50}$) in µM. The standard error is less than 5%. See the Supporting Information for additional details. [b] All 24 ADAMPs were also tested for hemolytic activity (as a measure of cytotoxicity) and found to be inactive up to 100 µM. [c] See Tables S5 and S6 in the Supporting Information for chemical properties (net charge, hydrophobicity, hydrophobic moment) and analytical characterization (HPLC, mass spectrometry) of all peptides. [d] Strains BL21DE3 (Novagen) and ATCC7468, respectively.
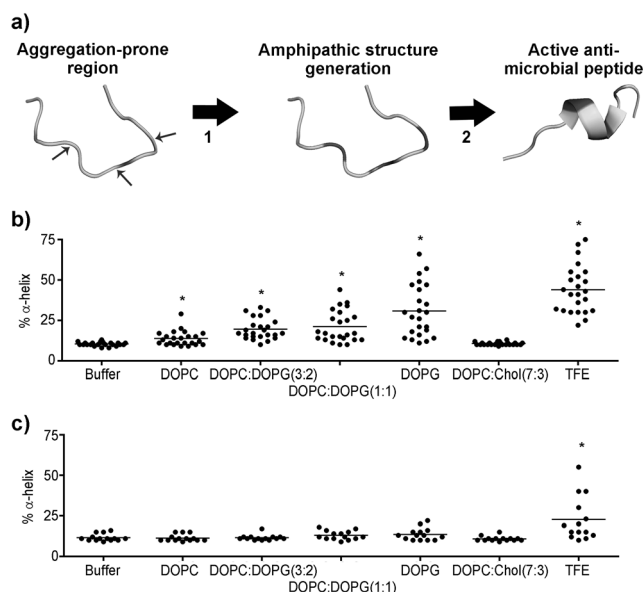

Figure 3. a) Putative amyloid-to-ADAMP transition. Amyloid-prone regions, predicted in Table S1 (Supporting Information), were cationized by Lys replacements (1) at positions 7, 12, and 15. ADAMPs are generally unstructured in solution but can adopt an α-helix conformation in hydrophobic environments such as bacterial membranes (2), with ensuing antimicrobial activity. b,c) Cirular-dichroism (CD) behavior of ADAMP and control peptides. The α-helical content of ADAMPs (b) and control peptides (c) under seven different conditions. The horizontal lines represent mean values. ADAMPs show increased levels of α-helix ($p < 0.005$) for TFE and membrane environments, in contrast to buffer or neutral (DOPC/cholesterol (Chol)), eukaryotic-like membranes. Control peptides show no such trend. DOPC = Dioleoyl-phosphatidylcholine, DOPG = Dioleoylphosphatidylglycerol.

activity, none of these peptides was found to be antimicrobial (Table 1).

In addition, as commonly found for typical AMPs, most ADAMPs underwent substantial α-helical structuration on switching from aqueous to hydrophobic environments such as 50% trifluoroethanol (TFE) or, more relevantly, to vesicles mimicking bacterial membranes, with structuration increasing with the content in anionic phospholipid (DOPG; Figure 3b). Interestingly, structuration was essentially nil in neutral, cholesterol-containing vesicles simulating eukaryotic membranes, thus supporting the notion that the well-known AMP selectivity for bacterial cells is directly related to differences in membrane lipid composition and fluidity[23] (Figure 3b).

In contrast, a panel of control peptides containing both random-generated and non-amyloid-derived sequences, with or without subsequent cationization, was conspicuously impervious to structuration upon similar environmental changes (Figure 3c). These results indicate that AMP evolution could only take place when eukaryote membranes had evolved to be robust enough to provide selectivity over microbial membranes against lytic AMPs.

In conclusion, our results show how antimicrobially active sequences can be generated from aggregation-prone regions of peptides and proteins, and thus hint at a plausible scenario for AMP emergence. Cationization at hot positions would be the mechanism whereby aggregation-prone regions are mutated into sequence stretches with the ability to adopt amphipathic structure (Figure 3a) and display antimicrobial activity upon contact with an appropriately lipophilic environment.

[1] Y. J. Gordon, E. G. Romanowski, A. M. McDermott, *Curr. Eye Res.* **2005**, *30*, 505–515.

[2] M. N. Melo, R. Ferre, M. A. Castanho, *Nat. Rev. Microbiol.* **2009**, *7*, 245–250.

[3] a) K. Matsuzaki, *Biochem. Soc. Trans.* **2001**, *29*, 598–601; b) Y. Shai, *Biochim. Biophys. Acta Biomembr.* **1999**, *1462*, 55–70.

[4] H. Zhao, R. Sood, A. Jutila, S. Bose, G. Fimland, J. Nissen-Meyer, P. K. Kinnunen, *Biochim. Biophys. Acta Biomembr.* **2006**, *1758*, 1461–1474.

[5] A. K. Mahalka, P. K. Kinnunen, *Biochim. Biophys. Acta Biomembr.* **2009**, *1788*, 1600–1609.

[6] A. J. Trexler, M. R. Nilsson, *Curr. Protein Pept. Sci.* **2007**, *8*, 537–557.

[7] M. R. Nilsson, C. M. Dobson, *Biochemistry* **2003**, *42*, 375–382.

[8] M. Torrent, F. Odorizzi, M. V. Nogues, E. Boix, *Biomacromolecules* **2010**, *11*, 1983–1990.

[9] a) C. Hertel, E. Terzi, N. Hauser, R. Jakob-Rotne, J. Seelig, J. A. Kemp, *Proc. Natl. Acad. Sci. USA* **1997**, *94*, 9412–9416; b) H. Zhao, E. K. Tuominen, P. K. Kinnunen, *Biochemistry* **2004**, *43*, 10302–10307.

[10] M. Stockl, P. Fischer, E. Wanker, A. Herrmann, *J. Mol. Biol.* **2008**, *375*, 1394–1404.

[11] E. E. Ambroggio, D. H. Kim, F. Separovic, C. J. Barrow, K. J. Barnham, L. A. Bagatolli, G. D. Fidelio, *Biophys. J.* **2005**, *88*, 2706–2713.

[12] S. J. Soscia, J. E. Kirby, K. J. Washicosky, S. M. Tucker, M. Ingelsson, B. Hyman, M. A. Burton, L. E. Goldstein, S. Duong, R. E. Tanzi, R. D. Moir, *PLoS One* **2010**, *5*, e9505.

[13] J. Miklossy, *J. Alzheimer's Dis.* **2008**, *13*, 381–391.

[14] E. Monsellier, M. Ramazzotti, N. Taddei, F. Chiti, *PLoS Comput. Biol.* **2008**, *4*, e1000199.

[15] A. P. Pawar, K. F. Dubay, J. Zurdo, F. Chiti, M. Vendruscolo, C. M. Dobson, *J. Mol. Biol.* **2005**, *350*, 379–392.

[16] M. Torrent, V. M. Nogues, E. Boix, *BMC Bioinf.* **2009**, *10*, 373.

[17] O. Conchillo-Sole, N. S. de Groot, F. X. Aviles, J. Vendrell, X. Daura, S. Ventura, *BMC Bioinf.* **2007**, *8*, 65.

[18] M. R. Yeaman, N. Y. Yount, *Nat. Rev. Microbiol.* **2007**, *5*, 727–740.

[19] P. Nicolas, *FEBS J.* **2009**, *276*, 6483–6496.

[20] K. A. Brogden, *Nat. Rev. Microbiol.* **2005**, *3*, 238–250.

[21] S. Lata, B. K. Sharma, G. P. Raghava, *BMC Bioinf.* **2007**, *8*, 263.

[22] S. Thomas, S. Karnik, R. S. Barai, V. K. Jayaraman, S. Idicula-Thomas, *Nucleic Acids Res.* **2010**, *38*, D774–D780.

[23] R. Sood, P. K. Kinnunen, *Biochim. Biophys. Acta Biomembr.* **2008**, *1778*, 1460–1466.